

Use of nanosecond corona discharge for generation of fine-disperse aerosol from organic vapors

S.P. Bugaev,¹ V.S. Kozlov,² A.V. Kozyrev,¹ M.V. Panchenko,²
and N.S. Sochugov¹

¹ Institute of High-Current Electronics,
Siberian Branch of the Russian Academy of Sciences, Tomsk

² Institute of Atmospheric Optics,
Siberian Branch of the Russian Academy of Sciences, Tomsk

Received May 12, 1999

We present some results of experimental investigation into the process of formation of the condensation aerosol from non-saturated styrene vapor in plasma of a pulsed corona discharge. It is shown that the characteristics of thus generated aerosol depend on the parameters of the discharge and the type of the carrier gas. The characteristic values of the aerosol particle number density and the volume median particle radius vary within respectively 10^7 – 10^8 cm⁻³ and 0.05–0.3 μm. We propose a model for the process of aerosol generation from the unsaturated vapor.

Introduction

It is well known that the presence of ions in a gas that contains vapor of a volatile liquid significantly speeds up the process of this liquid's vapor condensation. The ion-induced condensation of vapor, as a particular case of the heterogeneous condensation, plays a significant part in various atmospheric and technological processes. Therefore it is a subject for investigation for many research groups.^{1,2} Different sources of radioactive isotopes are usually used to produce ions. Negative and positive ions created in a gas become the condensation nuclei for molecules of the vapor, and thus nanometer-size aerosol particles are formed in the gas. To make the existence of neutral particles stable, the degree of supersaturation should increase with the decreasing radii of particle. For this reason small uncharged particles can steadily exist only in a sufficiently supersaturated vapor. At the same time, small charged particles also exist in unsaturated vapor.³

Effects associated with heterogeneous condensation of vapor molecules on ions, in particular, the formation of aerosol, can also manifest themselves in different types of electric discharges.^{4,5} Bogdanov has reported⁴ his measurement results on the mass concentration of aerosol formed in gaseous hydrocarbons under the action of an electron beam. These data evidence that formation of aerosol occurred in strongly unsaturated vapor of the radiolysis products of gaseous hydrocarbons. This follows, in particular, from the fact that after turning-off the source of irradiation (electron beam) the aerosol particles rapidly vaporize.

The presented results of our research into the interaction between the plasma of pulsed corona discharge and unsaturated vapor of different organic compounds show that aerosol particles are formed in such a plasma at low partial pressure of the vapor

(about 1% of the saturation pressure).⁶ We conducted the experiments with both aromatic (styrene, xylene, and others) and linear (q₅ – q₈) hydrocarbons. However, here we present only the experimental data obtained with styrene (q₆m₅q_m = q_{m2}). The use of styrene as a model organic admixture was mostly caused by its capability to polymerization. The low-temperature plasma acting on the styrene vapor can initiate the reactions of polymerization, while the formation of polymeric molecules leads to a decrease in the rate of vaporization of aerosol particles and to stabilization of the aerosol. Relative stability of particles allows us to apply the polarization nephelometric measurements of the aerosol optical characteristics to study such particles.

Our experiments were aimed at studying the main peculiarities in the process of formation of condensation aerosol (from the vapor of organic compounds in the recombining non-equilibrium plasma of a pulsed corona discharge under atmospheric pressure) at the stage when aerosol has already been formed. For this purpose we applied the approximate technique of optical diagnostics of particles. The corona discharge in these experiments was excited with high-voltage pulses of nanosecond duration. In this paper we demonstrate that by varying the electrophysical parameters of the generator of high-voltage pulses, the parameters of gas medium, and the initial concentration of vapor of a volatile substance in a gas it is possible to change the characteristics of the generated aerosol.

Experimental setup and the methods of diagnostics

Experimental setup

Figure 1 shows the block-diagram of the experimental setup. The principal part of the generator of high-voltage nanosecond pulses is the

binary beam-forming line, which is switched with two high-pressure gas-dischargers. The size of the beam-forming line governs the duration of a high-voltage pulse being 4 ns in our experiments. The maximum pulse repetition rate was 100 Hz; pulses of positive and negative polarity are generated alternatively. The amplitude of the output voltage is determined by the response thresholds of the gas-dischargers and can vary from 40 to 140 kV. The oscillograms of the positive and negative voltage pulses are shown in Fig. 2 as recorded at the pressure of 5.5 and 8 atm inside the gas-dischargers. The energy per pulse, calculated by integration of the oscillograms of the dropping voltage pulse, was 0.03 J. At the pulse repetition rate of 100 Hz this gives the mean power of 3 W.

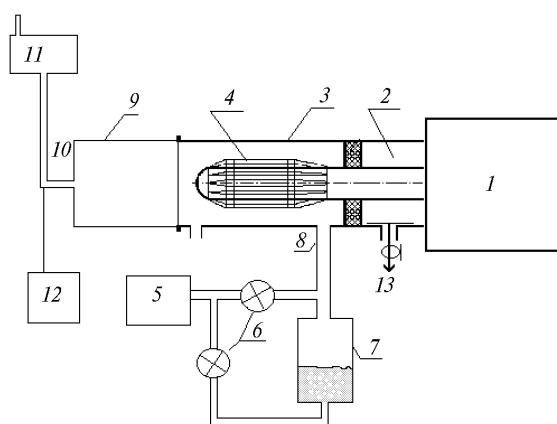


Fig. 1. The block-diagram of the experimental setup.

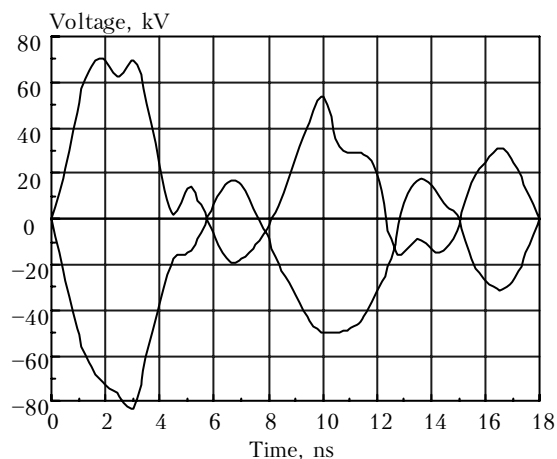


Fig. 2. Oscillograms of the voltage pulses of positive and negative polarity.

A high-voltage pulse from the generator 1 through the coaxial line 2 (see Fig. 1) with the wave impedance of 55Ω comes to the electrode system comprising a grounded cylindrical body 3 and high-voltage electrode 4 between which the corona discharge is excited. Because of a short duration of the exciting pulse, the discharge is of volume-diffuse character.

The gas pump through system consists of a pump 5, regulating valves 6, and the bubbler with a liquid hydrocarbon 7. The gas with a controlled content of vapor of an organic liquid enters through the inlet 8 and passes through the discharge zone where the process of aerosol formation is initiated. Then the gas flow comes into the aerosol chamber 9. The changeable volume of the aerosol chamber allows one to change (from 4 to 130 s) the delay between the time when the gas enters the discharge zone and the time the aerosol characteristics are measured in the optical cell of the FAN-type polarization nephelometer 11, to which the gas comes through the outlet 10 of the chamber. Some gas is sampled for analysis into the chromatograph 12. The amplitude of the voltage pulse is measured with the capacitance voltage divider 13.

The experiment was aimed at studying the influence of variations in principal parameters of the setup on the optical characteristics and, consequently, on the disperse composition of the aerosol generated. Among the factors influencing these aerosol parameters we consider the principal parameters of the setup that determine the discharge energy and concentration of unsaturated vapor. From the methodical viewpoint it is important to note that the generation of aerosol and optical measurements ran under conditions of low relative air humidity in the gas pipelines of the setup (below 30%). This allowed us to eliminate the influence of this factor and to use fixed values of optical constants of the particulate matter for styrene particles when interpreting the results. Besides, the sink of styrene particles onto the walls of the aerosol chamber and gas pipelines can likely play a certain part in variation of the number density of styrene particles. However, in our opinion, this may not significantly change the sought qualitative peculiarities in the influence of the parameters of experiment on the characteristics of aerosol. Conceivably this point could be a subject for our further investigations.

Variations of the discharge energy parameters

The measurements were performed in the pump through mode. Pure air or argon was used as a carrier gas of unsaturated vapor. The carrier gas (with the volume flow rate $Q = 250 - 600 \text{ l/h}$) was mixed with the styrene vapor (bubbling with mass consumption $l_s = 0.16 - 0.75 \text{ g/h}$). The gas entered the discharge zone of the generator of nanosecond pulses (pulse repetition rate $f = 33, 50, \text{ or } 100 \text{ Hz}$, that is, the discharge power $W = 1, 1.5, \text{ or } 3 \text{ W}$). The corona high-voltage electrode was made of thin wires put along the discharge chamber. As the number of wires changed, the total power absorbed by the discharge practically did not change, therefore the volume energy density in the discharge zone and the concentration of ions varied roughly proportional to the number of corona wires.

Analysis of chemical composition of the gas mixture

In the experiments the gravimetric measurements of the styrene mass consumption was performed at the entrance into the discharge chamber l_0 (g/m³). To detect chemical changes in the vapor-gas mixture composition, gaseous components were analyzed by chromatographic methods at the chamber entrance and exit. The concentration and chemical composition of the admixture at the entrance and exit were determined with the plasma ionization detector of an I 4700 chromatograph. The 3-m long chromatographic column with OV-101 sorbent was used. Distillation was performed in the isothermal mode.

Optical diagnostics of aerosol

Optical characteristics and disperse composition of aerosol particles were studied by the polarization nephelometry of scattered radiation. This method is one of the most sensitive methods for studying the

dynamics of fine-disperse aerosol.⁷⁻⁹ It should be noted that the polarization nephelometry for the visible spectral region with the scattering angles varying from 10 to 170° is informative, first of all, relative to the parameters of the fine aerosol fraction (particles with radii from 0.05 to 0.5 μm), because it is just these particles that primarily determine the optical properties of aerosol in the visible spectral region.⁷ In this connection, the nephelometric instrumentation and measurement technique used in this work allow the composition of styrene aerosol to be studied only at a sufficiently "late" stage when optically active particles are already formed. The direct study of earlier stages of aerosol formation (clusterization and others) cannot be done with the optical technique utilized in this experiment. The data analyzed here correspond to the time of aerosol "aging," which is determined by the geometrical parameters of the measuring device (separation of the FAN optical cell from the discharge zone and the volume of the aerosol chamber of the generator), in the interval from 4 to 130 s. Mostly the measurements were performed at a fixed time of aging equal to 4 s (Table 1).

Table 1. Optical and microstructure parameters of styrene aerosol.

| No. | Carrier gas | W, W | M ₀ , g/m ³ | σ ₁ , m ⁻¹ (λ = 0.41 μm) | σ ₂ , m ⁻¹ (λ = 0.50 μm) | σ ₃ , m ⁻¹ (λ = 0.63 μm) | P ₁ , % | P ₂ , % | P ₃ , % | a _{0V} , μm | S ² | N, cm ⁻³ · 10 ⁷ | γ _a , % |
|---------------------|-------------|------|-----------------------------------|--|--|--|--------------------|--------------------|--------------------|----------------------|----------------|---------------------------------------|--------------------|
| 1 | Air theor. | 1 | 0.41 | 0.165 | 0.100 | 0.066 | 51 | 60 | 77 | 0.091 | 0.2 | 2.06 | 5.8 |
| | | | | 0.174 | 0.100 | 0.058 | 50 | 64 | 76 | | | | |
| 2 | Air theor. | 1 | 2.96 | 1.05 | 0.676 | 0.850 | 28 | 43 | 65 | 0.126 | 0.1 | 2.49 | 4.0 |
| | | | | 1.32 | 0.876 | 0.600 | 27 | 43 | 64 | | | | |
| 3 | Air theor. | 3 | 0.41 | 0.334 | 0.190 | 0.143 | 34 | 45 | 64 | 0.115 | 0.2 | 1.43 | 8.0 |
| | | | | 0.322 | 0.225 | 0.127 | 33 | 46 | 64 | | | | |
| 4 | Air | 3 | 2.96 | 4.40 | 4.00 | 4.70 | 4 | 12 | 29 | 0.189 | 0.3 | 8.05 | 17.8 |
| 5 | Air | 3 | 3.0 | 2.27 | 1.76 | 1.90 | 0 | 6 | 20 | 0.251 | 0.5 | 4.07 | 8.4 |
| 6 | Argon | 3 | 2 | 17.1 | 12.9 | 14.0 | -12 | -6 | 4 | 0.295 | 0.3 | 6.79 | 87.7 |
| Limiting variations | | 1 | 0.4 | 0.12 | 0.07 | 0.04 | -15 | -10 | 0 | 0.09 | 0.1 | 0.59 | 2 |
| | | 3 | 3 | 17 | 13 | 14 | 50 | 60 | 80 | 0.30 | 0.6 | 15 | 88 |

The FAN-type polarization pump through nephelometer was used to measure the coefficients of aerosol scattering μ_λ(45°) at the scattering angle φ = 45° and polarization components of the scattering phase function μ_{1λ}(90°) and μ_{2λ}(90°) at three wavelengths λ = 0.41, 0.50, and 0.63 μm. Here μ_{1λ} and μ_{2λ} are the orthogonal linearly polarized components of the scattering phase function with the electric vector perpendicular and parallel to the scattering plane, respectively. They allow calculation of the spectral values of the degree of polarization of radiation scattered at the angle of 90°:

$$P_λ(90°) = (μ_{1λ} - μ_{2λ}) / (μ_{1λ} + μ_{2λ}) .$$

To measure the scattering coefficient in absolute units (m⁻¹ · sr⁻¹), the device was first calibrated by gases according to the technique described in Ref. 10. The values of the aerosol scattering coefficients σ_λ (m⁻¹) were determined from the ratio

σ_λ = μ_λ(45°) / μ_{nλ}(45°), where μ_{nλ}(45°) are the values of the normalized scattering phase function estimated from the results of inversion of optical measurement data.

Analysis of the results of multiple measurements has revealed high reproducibility of the optical characteristics and, consequently, parameters of the generated aerosol in time at the fixed parameters of the measurement scheme (geometrical parameters of the setup, characteristics of the pulsed corona discharge, concentration of organic vapor, type of the carrier gas). This allowed us to study by turn the influence of the above-mentioned dynamic factors on the variability of aerosol characteristics. Each individual realization of the experiment presented in Table 1 was estimated from the data of two or three measurement series conducted during 15 to 30 min. For this time interval the relative variability of optical characteristics did not exceed, on the average, 10–15%. This is indicative of high stability of the parameters of aerosol generated in each particular experiment and, on

the whole, of good performance of the setup as a generator of aerosol.

In the methodical aspect, the influence of multiple scattering effect on the results of optical measurements can be neglected because of small linear dimensions of the FAN scattering volume. In this case, for the time of 10 s, during which every individual optical characteristic was recorded, at the pump through rate about 10 l/min the scattering volume of aerosol about 1.5 liter is analyzed. At a high concentration it is sufficient for adequate presentation of fine aerosol particles generated in the pulsed corona discharge.

The polarization nephelometric measurements were used to determine the parameters of aerosol in the approximation of unimodal lognormal size-distribution of homogeneous spherical particles:

$$dN(a) = N(\sqrt{2\pi}aS)^{-1} \exp(-\ln^2(a/a_0)/2S^2) da, \quad (1)$$

where $dN(a)$ is the number of particles in the interval of radii from a to $a + da$; N is the total number density; a_0 is the geometrical mean (median) radius of particles; S^2 is the variance of the logarithm of radii.

The investigations performed for the atmospheric aerosol and different aerosols of condensation nature (see, for example, Refs. 7–9) showed that single-peak lognormal distributions of the type (1) well describe the particle size-distribution of the fine-disperse fraction and allow simulation of optical properties of aerosols. At the same time, for some condensation aerosols, which are characterized, during formation, by intense processes of heterogeneous condensation of aerosol forming vapor and coagulation of particles, the second narrow mode may arise in the size range 0.3–0.5 μm along with the main fine-disperse mode.⁹ We observed such manifestations of a more complicated structure of the size spectrum in peculiar features of the aerosol optical properties (nonmonotonic spectral behavior of the scattering coefficient, see Table 1) in the studied process of aerosol generation. Under such conditions, the single-peak size-distribution function is the first approximation for estimating the parameters of the particle size-distribution of the fine-disperse aerosol fraction. The approximate microstructure estimates allow us, in this case, to study principal qualitative regularities of the variability of styrene aerosol under the action of different factors.

Microstructure characteristics of particles, with known optical constants of the particulate matter, were determined by fitting the calculated spectral dependences to the measured ones for the degree of polarization and scattering coefficient. For calculations we used the lognormal size-distributions of homogeneous spherical particles in the single-scattering approximation.¹¹ Note that such methods of microstructure estimates^{12,13} are not exactly the inversion methods.¹⁴ However, they are used rather often and provide for obtaining quite good results.

The main purpose of inverting optical measurements was to determine parameters of the aerosol disperse composition (microstructure). In calculations we used the corresponding literature data on the styrene refractive index $n = 1.55$ and absorption coefficient $\chi = 0$. Note that these values of optical constants are practically the same for styrene and other products of its conversion found in the experiment. The median radius a_0 (in μm), variance S^2 , and the particle number density N (in cm^{-3}) were estimated numerically.

The estimates were done in the following order. First, we used the measured spectral dependence of the degree of polarization to determine the characteristics of size-distribution function S^2 and the particle median radius a_0 . In so doing, we used the calculated dependence of the degree of polarization on the volume median particle radius a_{0V} (this diagram is very convenient for practical use).¹² Then the measured values of scattering coefficient (taking into account the calculated values of the normalized scattering phase function and normalized, to the number density, scattering coefficient) were used to estimate the particle number density N . The aerosol parameters a_0 and N were determined separately for each wavelength, and thus obtained values were averaged. With known parameters of the size-distribution function we can calculate such important generalized parameters as the cubic mean radius a_3 and the median volume radius a_{0V} :

$$a_3 = a_0 \exp(3S^2/2), \quad (2)$$

$$a_{0V} = a_0 \exp(3S^2). \quad (3)$$

The mass concentration of the aerosol $M_V(\text{g}/\text{m}^3)$ can be determined through the cubic mean radius a_3 and particle number density N as

$$M_V = (4/3)\pi a_3^3 \rho N = (4/3)\pi a_0^3 \rho N \exp(9S^2/2), \quad (4)$$

where ρ , in g/cm^3 , is the density of the particulate matter. As was shown in Ref. (12), the volume median particle radius a_{0V} is the effective generalized parameter, which well describes the influence of each of the two parameters, a_0 and S^2 , on the angular characteristics of light scattering. Finally, the estimated mass concentrations allowed us to determine the coefficient of aerosol yield at the aerosol formation:

$$\gamma_a = M_V/M_0. \quad (5)$$

The results of inversion of optical measurements (see Table 1) show that the estimated parameters of particles allow reconstruction of the degree of linear polarization accurate to 1–3%. The relative error in reconstructing the aerosol scattering coefficient, which actually corresponds to the error in determination of the particle number density, is on average about 20–30%. Table 1 gives some results of comparison of the

measured and reconstructed (calculated) data (rows 1–3). They indicate that the use of a unimodal particle size distribution function allows an adequate description of the optical characteristics of aerosol.

Experimental results

The conducted experiments have shown that the characteristics of aerosol generated in the pulsed corona discharge zone strongly depend both on the electrophysical parameters of the discharge (pulse repetition rate, ion density in the discharge zone, geometry of the discharge zone) and on the type of the carrier gas.

It should also be expected that the conditions of aerosol formation in air and argon differ significantly because the oxygen in air inhibits the reactions of polymerization and gum formation. The oxidation reactions running in the oxygen-containing atmosphere must result in formation of a wide variety of products of incomplete styrene oxidation in the resulting gas

and (or) in a decrease of the concentration of the organic admixture due to reactions of complete oxidation.

Analysis of the influence of dynamic factors has shown that each of them affects the dynamics of aerosol composition in its own way. Thus, that or another composition of aerosol can be generated and studied. On the whole, the scattering coefficients, mass concentration, and particle number density can vary by ten times and even more.

Influence of the carrier gas and vapor concentration on the parameters of aerosol

Chromatographic studies of the admixture composition in the resulting gas were conducted for air and argon as a carrier gas, all other factors being the same. The results of these studies are presented in Table 2 along with the main characteristics of the aerosol. One can see that the characteristics of aerosol formed in air and argon differ markedly.

Table 2. Data of a comparison between the aerosol characteristics generated in the air and argon

| Gas | Q, l/h | M ₀ , g/m ³ | W, W | Composition and content of the organic admixture in the resulting gas, g/m ³ | | | Characteristics of the aerosol | | | |
|-------|--------|-----------------------------------|------|---|--------------|-------------------|--------------------------------|---------------------|-----------------------------------|----------------|
| | | | | Styrene | Benzaldehyde | Polymers and gums | a ₀ , μm | N, cm ⁻³ | M _V , g/m ³ | S ² |
| Air | 250 | 1.35 | 3 | 0 | 0.33 | 0 | 0.044 | 4.3·10 ⁷ | 0.22 | 0.6 |
| Argon | 250 | 1.60 | 3 | 0.55 | 0.34 | 0.30 | 0.108 | 7.6·10 ⁷ | 1.45 | 0.3 |

The aerosol formed in the argon atmosphere is denser. Its mass concentration exceeds by roughly seven times that of the aerosol formed in the air, while the number density is almost twice as large as that in the air. The particle size of aerosol obtained in argon is also larger. Note that the disbalance between the mass concentration of the styrene admixture in the initial gas (1.6 g/m³) and the summed mass concentration of the admixtures in the processed gas (1.19 g/m³). This can be explained by the presence of polymerized products or gums which cannot be detected by the employed method in the processed gas. A noticeable fraction of the styrene content experienced oxidation to benzaldehyde (q_{6m5qmn}) due to the presence of oxygen in argon. For the example presented in Table 2, the coefficient of aerosol formation is 90%, that is, a noticeable amount of styrene and benzaldehyde is found in the condensed state. The measured concentration of styrene and benzaldehyde made 2.5 and 7.5% of the concentration of saturated vapor under the experimental conditions.

The process of aerosol formation in the air differs significantly from the above-considered in the case of the argon atmosphere. The chromatographic analysis showed that the resulting gas contained only one organic admixture, which was identified as benzaldehyde. The benzaldehyde concentration made up to 7% of the concentration of saturated vapor. Styrene

in the resulting gas was detected only in trace amounts. The absence of high polymer traces in the chromatograms shows that styrene polymerization and gum formation did not occur. A large amount of styrene molecules has experienced complete oxidation to water and carbon dioxide. This is quite characteristic of such plasmochemical processes. Although the coefficient of aerosol yield relative to the initial concentration of styrene was only 16%, 67% of the admixture detected by the chromatographic methods was in the condensed state.

Table 1 gives some data on optical and microstructure characteristics of aerosol for different parameters of the experiment. Typical values of the aerosol particle number density *N* are of the order of 10⁷–10⁸ cm⁻³, while the scattering coefficients *y* are characterized by the visibility range varying within 0.3–50 m. The disperse composition of aerosol particles varies from fine quasimonodisperse distributions with the variance *S*² = 0.1 to a wide (*S*² = 0.5–0.6) coarse-disperse distributions. In this case the median particle radius *a*₀ changes by more than three times. Variations of the degree of polarization are also large *p*₂ = (-0.11)–(+0.6). The coefficient of aerosol formation *γ*_a described by Eq. (5) varies from low values to almost complete gas–particle conversion: 1.8–90%.

The gas composition of the atmosphere (carrier gas) has a decisive effect on the coefficient of aerosol formation. In the air atmosphere the upper limit of *γ*_a

variations is 15–20%, whereas in the atmosphere of a noble gas (argon) the aerosol yield exceeds 30% and can reach 90%.

Variation of the initial concentration (partial pressure) M_0 of styrene vapor produces a marked effect on the process of aerosol formation: increase in the content of styrene vapor results in formation of larger aerosol particles, densening of the aerosol medium, and some growth of the coefficient of aerosol formation (see Table 1).

Influence of the gas discharge characteristics on the parameters of aerosol

To study dependence of aerosol characteristics on the concentration of plasma ions, we have conducted the experiments with different designs of the discharge chamber. While keeping constant the discharge power and varying the number of corona electrodes, we have changed the concentration of plasma in the pulsed corona discharge zone. Figure 3 shows the dependences of the aerosol parameters on the concentration of plasma ions in the discharge n , in cm^{-3} , (Fig. 3a) and the power absorbed in the discharge, W (Fig. 3b).

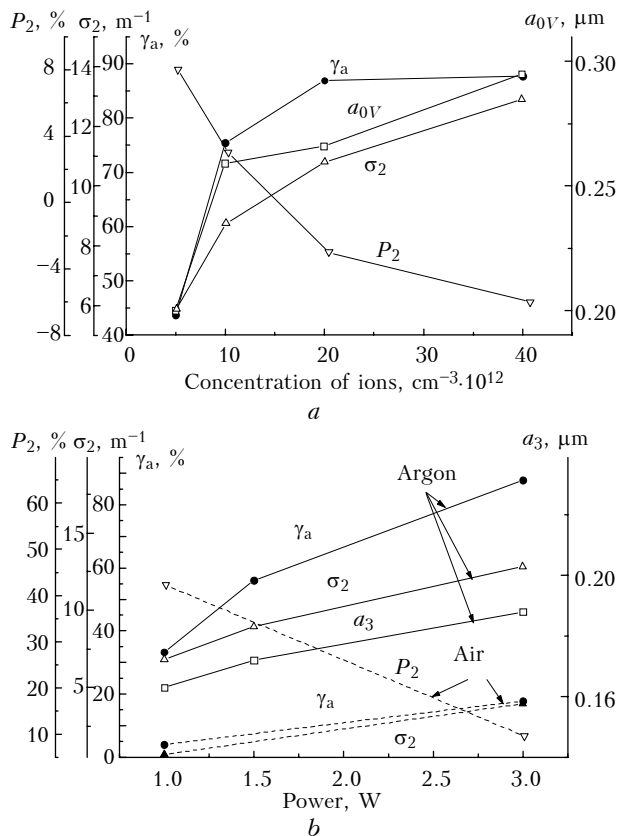


Fig. 3. Variability of the optical characteristics and aerosol microstructure vs. the concentration of ions (a) and the power of the corona discharge (b): (a) argon, $Q = 250$ l/h, $M_0 = 1.6$ g/ m^3 , $W = 3$ W; (b) argon, $Q = 250$ l/h, $M_0 = 2.2$ g/ m^3 ; air, $Q = 250$ l/h, $M_0 = 3$ g/ m^3 .

These dependences indicate that the increase in n and W favors a more intense formation of aerosol. Besides,

this effect is characterized by a significant increase in the coefficient of aerosol formation and growth of aerosol particles in size.

Evolution of aerosol

Figure 4 shows the dependences, which characterize the change of parameters with the varying distance from the zone of generation due to increasing volume and length of the aerosol chamber. Aerosol evolution in the time interval from 4 to 130 s closely follows the coagulation transformation of particles. The aerosol particle number density decreases with time by about an order of magnitude, while the aerosol particles become almost twice as large. At the same time, the aerosol yield and scattering coefficients change only slightly.

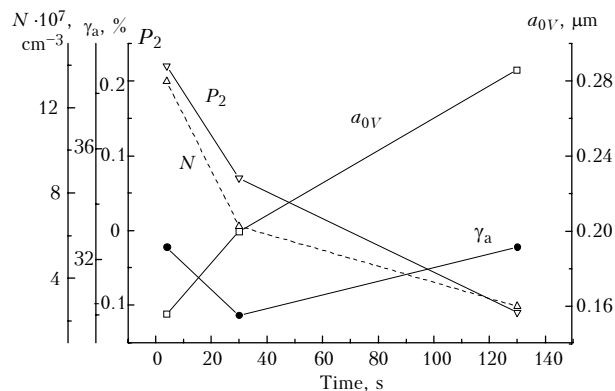


Fig. 4. Evolution of optical characteristics and disperse composition of aerosol: argon, $Q = 250$ l/h, $M_0 = 2.1$ g/ m^3 , $W = 3$ W.

Mechanism of formation of aerosol particles in plasma

To explain the effect of aerosol formation from unsaturated vapor, we propose the following mechanism of condensation of unsaturated vapor in plasma. The pulsed corona discharge generates positive and negative ions in a gas (mostly n_2^- and N_2^+).¹⁵ These ions serve the centers of heterogeneous condensation thus leading to formation of particles with the characteristic size of fractions being within the nanometer range.³ The number of molecules condensed on one ion varies from 10 to 30. The concentration of styrene molecules in air is about 10^{16} cm^{-3} , and the initial concentration of plasma of the pulsed corona discharge is about 10^{13} cm^{-3} . Thus, about 10^{14} cm^{-3} admixture molecules are condensed on ions generated by a single pulse of the corona discharge. If the pulse repetition rate is 100 Hz and the gas is in the discharge zone for 5 s, all vapor molecules can be condensed on charged particles. The further growth of particles is due to their coagulation under the action of Coulomb's attraction force and as a result of chaotic thermal motion.

Figure 5 demonstrates the theoretically estimated evolution of the characteristic size of aerosol particles for the three values of l_0 : $l_0 = 0.5, 1.0,$ and 2.0 g/m^3 . These estimates were obtained within the framework of a simplified model of coagulation ignoring the process of drop evaporation.¹⁶

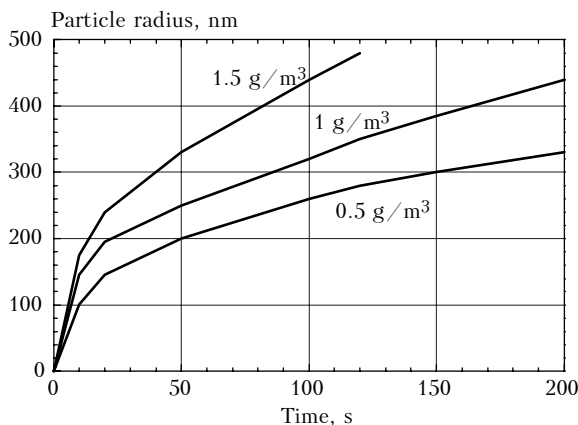


Fig. 5. Calculated evolution of the particle radius for different concentration of the vapor mixture.

According to these estimates, the particles entering the measuring chamber should have the radius about 150 nm by 8 to 10 seconds after they left the discharge zone. The experimentally obtained characteristic size of aerosol particles well correlates with the calculated results obtained when completely neglecting the evaporation rate. This suggests that the evaporation process may actually occur to be slow. This point of view is also supported by the results of comparative experiments with the condensation of hexane and alcohol vapor. In this case the aerosols were less optically dense than the styrene aerosol, although all other parameters of the substance (density, pressure of saturated vapor, evaporation heat) are close to that of styrene. The principal difference is likely due to the capability of liquid styrene to polymerization and gum formation. Taking into account this point, we can suggest the following explanation to the experiments.

The mechanism of particle formation is caused by heterogeneous condensation of molecules of unsaturated vapor on plasma ions with their subsequent growth due to recombination and coagulation. However, under the exposure to UV radiation from the discharge or under the action of radicals generated by the discharge, the styrene particles are subjected to a fast partial polymerization or gum formation. Polymerization and gum formation are probably of predominantly surface character thus preventing evaporation of particles as they closely approach each other. For this reason the particles grow to a relatively large size.

It is important to note that particle evaporation does not slow down the process of charge recombination in the medium. The rate of recombination of ions and the rate of coagulation of particles are almost the same, while the rate of recombination in the presence of vapor of substances that are incapable of polymerizing far exceeds the rate of particle growth. In the latter case, charges recombine, while the particle size may remain unchanged.

Conclusions

The above discussed research allows us to reveal and study the peculiarities in formation and transformation of the aerosol generated due to interaction of unsaturated styrene vapor with the plasma of the pulsed corona discharge. The influence of dynamic factors (carrier gas, vapor concentration, gas discharge characteristics) on the efficiency of the process of aerosol formation has been analyzed in detail.

The proposed mechanism of growth of aerosol particles is close to the mechanism usually used to describe the process of formation of disperse phase at relaxation of aerosol plasma containing solid particles. However, in the above-considered case, the condensing vapors of all substances are unsaturated. So the condensation process is non-equilibrium in principle. Formation of the metastable condensed phase becomes possible only if the rate of condensation exceeds the rate of evaporation. In our case, fulfillment of this condition fully depends on the presence of recombining charges in the condensation zone. Thus, the condensation of unsaturated vapor has the character of a process stimulated by recombining low-temperature plasma.

The experimental setup used in this work can be proposed as an easy-to-operate stable generator of condensation aerosol with a controlled composition. It enables one to change the disperse composition and mean size of aerosol particles in a wide range.

References

1. Jr.A.W. Castleman, *Space Sci. Rev.* **15**, 547–589 (1974).
2. T.O. Kim, M. Adachi, K. Okuyama, and J.H. Seinfeld, *J. Aerosol. Sci.* **26**, 527–543 (1997).
3. N.N. Das Gupta and S.K. Ghosh, *Rev. Modern Phys.* **18**, 225–290 (1946).
4. V.S. Bogdanov, *Dokl. Akad. Nauk SSSR* **136**, 121–124 (1961).
5. H.-R. Paur, H. Matzing, and K. Woletz, *J. Aerosol Sci.* **22**, 509–512 (1991).

6. S.P. Bugaev, A.V. Kozyrev, N.S. Sochugov, and P.A. Khryapov, in: *Proc. of 13th International Symposium on Plasma Chemistry* (Beijing, China, 1997), pp. 825–829.
7. G.V. Rozenberg, G.I. Gorchakov, Yu.S. Georgievskii, and Yu.S. Lyubovtseva, in: *Physics of the Atmosphere and Problems of Climate* (Nauka, Moscow, 1980), pp. 216–257.
8. M.V. Kabanov, M.V. Panchenko, Yu.A. Pkhalagov, V.V. Veretennikov, V.N. Uzhegov, and V.Ya. Fadeev, *Optical Properties of Coastal Atmospheric Haze* (Nauka, Novosibirsk, 1988), 201 pp.
9. V.S. Kozlov and M.V. Panchenko, *Fiz. Goreniya i Vzryva* **32**, No. 5, 122–133 (1996).
10. M.V. Panchenko, A.G. Tumakov, and S.A. Terpugova, in: *Equipment for Remote Sensing of Atmospheric Parameters* (Institute of Atmospheric Optics of Siberian Branch of the Academy of Sciences of the USSR, Tomsk, 1987), pp. 40–46.
11. V.S. Kozlov and V.Ya. Fadeev, “*Tables of Optical Scattering Characteristics of Fine-Disperse Aerosol with the Lognormal Size-Distribution Function*,” Preprint No. 30, Institute of Atmospheric Optics of Siberian Branch of the Academy of Sciences of the USSR, Tomsk, 1981), 66 pp.
12. V.S. Kozlov, “*Experimental Studies of Optical and Microphysical Properties of Smoke Aerosols*,” Cand. Phys. Math. Sci. Dissert., Tomsk (1985), 234 pp.
13. V.V. Lukshin and A.S. Isakov, *Izv. Akad. Nauk SSSR, Fiz. Atmos. Okeana* **24**, 250–257 (1988).
14. V.E. Zuev and I.E. Naats, *Inverse Problems of Laser Sounding of the Atmosphere* (Nauka, Novosibirsk, 1982), 242 pp.
15. Yu.P. Raizer, *Physics of Gas Discharge* (Nauka, Moscow, 1987), 592 pp.
16. C.P. Bugaev, A.V. Kozyrev, V.A. Kuvshinov, and N.S. Sochugov, *Dokl. Akad. Nauk* **361**, 612–615 (1998).